Optimal Scan Strategies for Material Decomposition in Photon-Counting CT with Multiple Contrast Agents

Stefan Sawall, Edith Baader, and Marc Kachelrieß

German Cancer Research Center (DKFZ)
Heidelberg, Germany
www.dkfz.de/ct

Proposals to Simultaneously use More than One Contrast Agent

1. J. Schlomka, E. Roessl, R. Dorscheid, S. Dill, G. Martens, T. Istel, C. Baumer, C. Herrmann, R. Steadman, G. Zeitler, A. Livne, and R. Proksa. Experimental Feasibility of Multi-Energy Photon-Counting K-Edge Imaging in Pre-Clinical Computed Tomography. Phys. Med. Biol. 53, 4031-4047 (2008).
2. D. P. Cormode, E. Roessl, A. Thran, T. Skajaa, R. E. Gordon, J.-P. Schlomka, V. Fuster, E. A. Fisher, W. J. M. Mulder, R. Proksa, and Z. A. Fayad. Atherosclerotic Plaque Composition: Analysis with Multicolor CT and Targeted Gold Nanoparticles. Radiology 256, 774-782 (2010).
3. J. Mongan, S. Rathnayake, Y. Fu, R. Wang, E. F. Jones, D.-W. Gao, and B. M Yeh. In Vivo Differentiation of Complementary Contrast Media at Dual-Energy CT. Radiology 265, 267-272 (2012).
4. M. Qu, E. Ehman, J. G. Fletcher, J. E. Huprich, A. K. Hara, A. C. Silva G. Farrugia, P. Limburg, and C. H. McCollough. Toward Biphasic Computed Tomography (CT) Enteric Contrast: Material
5. Classification of Luminal Bismuth and Mural Iodine in a Small-Bowel Phantom Using Dual-Energy CT. Journal of Computer Assisted Tomography 36, 554-559 (2012).
6. D. P. Clark, K. Ghaghada, E. J. Moding, D. G. Kirsch, and C. T. Badea. In Vivo Characterization of Tumor Vasculature using Iodine and Gold Nanoparticles and Dual Energy Micro-CT. Phys. Med. Biol. 58, 1683-1704 (2013).
7. J. R. Ashton, D. P. Clark, E. J. Moding, K. Ghaghada, D. G. Kirsch, J. L. West, and C. T. Badea. Dual-Energy Micro-CT Functional Imaging of Primary Lung Cancer in Mice Using Gold and Iodine Nanoparticle Contrast Agents: A Validation Study. PLoS ONE 9, e88129 (2014).
8. S. Rathnayake, J. Mongan, A. S. Torres, R. Colborn, D.-W. Gao, B. M. Yeh, and Y. Fu. In Vivo Comparison of Tantalum, Tungsten, and Bismuth Enteric Contrast Agents to Complement Intravenous Iodine for Double-Contrast Dual-Energy CT of the Bowel: Enteric Contrast Comparison for Dual-Energy CT of the Bowel. Contrast Media & Molecular Imaging 11, 254-261 (2016).
9. D. P. Cormode, S. Si-Mohamed, D. Bar-Ness, M. Sigovan, P. C. Naha, J. Balegamire, F. Lavenne, P. Coulon, E. Roessl, M. Bartels, M. Rokni, I. Blevis, L. Boussel, and P. Douek. Multicolor Spectral Photon-Counting Computed Tomography: in Vivo Dual Contrast Imaging with a High Count Rate Scanner. Scientific Reports 7, 4784 (2017).
10. R. Symons, T. E. Cork, M. N. Lakshmanan, R. Evers, C. Davies-Venn, K. A. Rice, M. L. Thomas, C.-Y. Liu, S. Kappler, S. Ulzheimer, V. Sandfort, D. A. Bluemke, and A. Pourmorteza, Dual-Contrast Agent Photon-Counting Computed Tomography of the Heart: Initial Experience. The International Journal of Cardiovascular Imaging 33, 1253-1261 (2017).
11. R. Symons, B. Krauss, P. Sahbaee, T. E. Cork, M. N. Lakshmanan, D. A. Bluemke, and A. Pourmorteza. Photon-Counting CT for Simultaneous Imaging of Multiple Contrast Agents in the Abdomen: An in Vivo Study, Med. Phys. 44, 5120-5127 (2017).
12. R. Symons, B. Krauss, P. Sahbaee, T. E. Cork, M. N. Lakshmanan, D. A. Bluemke, and A. Pourmorteza. Photon-Counting CT for Simultaneous Imaging of Multiple Contrast Agents in the Abdomen: An in Vivo Study. Med. Phys. 44, 5120-5127 (2017).
13. D. Muenzel, D. Bar-Ness, E. Roessl, I. Blevis, M. Bartels, A. A. Fingerle, S. Ruschke, P. Coulon, H. Daerr, F. K. Kopp, B. Brendel, A. Thran, M. Rokni, J. Herzen, L. Boussel, F. Pfeiffer, R. Proksa, E. J. Rummeny, P. Douek, and P. B. Noël. Spectral Photon-Counting CT: Initial Experience with Dual-Contrast Agent K-Edge Colonography. Radiology 283, 723-728 (2017).
14. D. Muenzel, H. Daerr, R. Proksa, A. A. Fingerle, F. K. Kopp, P. Douek, J. Herzen, F. Pfeiffer, E. J. Rummeny, and P. B. Noël, Simultaneous Dual-Contrast Multi-Phase Liver Imaging using Spectral
15. Photon-Counting Computed Tomography: a Proof-of-Concept Study. European Radiology Experimental 1, 25 (2017).
16. J. Dangelmaier, D. Bar-Ness, H. Daerr, D. Muenzel, S. Si-Mohamed, S. Ehn, A. A. Fingerle, M. A. Kimm, F. K. Kopp, L. Boussel, E. Roessl, F. Pfeiffer, E. J. Rummeny, R. Proksa, P. Douek, and P. B. Noël. Experimental Feasibility of Spectral Photon-Counting Computed Tomography with Two Contrast Agents for the Detection of Endoleaks Following Endovascular Aortic Repair,.European Radiology 28, 3318-3325 (2018).
17. I. Riederer, D. Bar-Ness, M. A. Kimm, S. Si-Mohamed, P. B. Noël, E. J. Rummeny, P. Douek, and D. Pfeiffer. Liquid Embolic Agents in Spectral X-Ray Photon-Counting Computed Tomography using Tantalum K-Edge Imaging. Scientific Reports 9, 5268 (2019).
18. T. C. Soesbe, M. A. Lewis, K. Nasr, L. Ananthakrishnan, and R. E. Lenkinski. Separating High-Z Oral Contrast from Intravascular Iodine Contrast in an Animal Model using Dual-Layer Spectral CT, Academic Radiology 26, 1237-1244 (2019).
19. L. Ren, K. Rajendran, J. G. Fletcher, C. H. McCollough, and L. Yu, Simultaneous Dual-Contrast Imaging of Small Bowel with Iodine and Bismuth using Photon-Counting-Detector Computed Tomography: a Feasibility Animal Study. Investigative Radiology 55, 688-694 (2020).
20. … many more (also at this AAPM meeting) …

dkfz.

Aim

- PCCT can distinguish more than two materials.
- Is it good to use two contrast agents, X and Y, simultaneously?
- What is to be preferred?
  - A single scan such as WXY
  - Two or even three scans, such as WX+WY or W+WX+WY
- Assumption: Zero motion
- Task: Material decomposition

e.g. iodine (X) *e.g. hafnium* (Y)

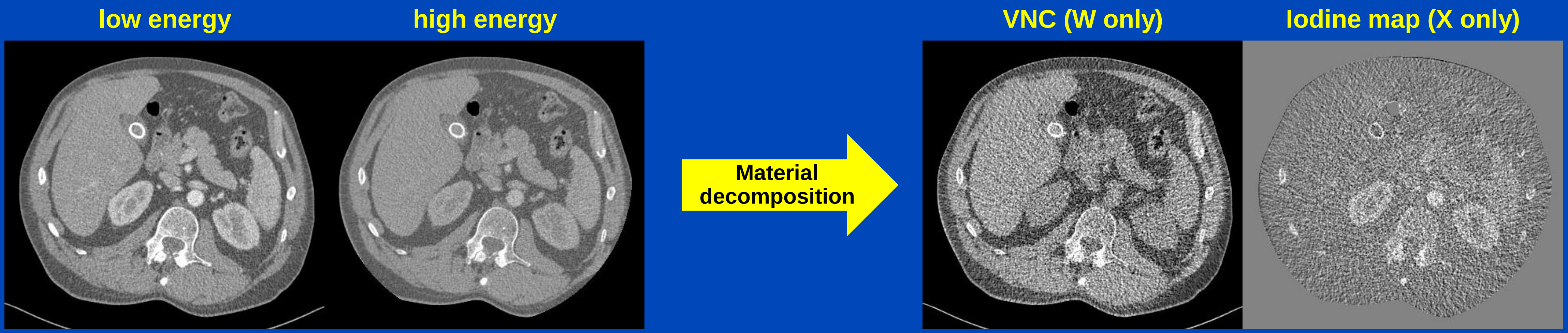

Why is Subtraction Potentially Better?
(in case of no motion)

- W = soft tissue (water) signal, X = iodine signal
- Assume same noise N, e.g. 50 HU, in both measurements M_1 and M_2
  - Var M_1 = Var M_2 = N^2 regardless of whether iodine is present or not
- DECT
  - Measurement 1 (high kV): $M_1 = W + 0.25\,X$
  - Measurement 2 (low kV): $M_2 = W + 0.5\,X$
  - Estimated iodine: $4\,(M_2 - M_1)$ Variance = 16 (Var M_2 + Var M_1) = 32 N^2
  - Estimated soft tissue: $2\,M_1 - M_2$ Variance = 4 Var M_1 + Var M_2 = 5 N^2
- Subtraction
  - Measurement 1 (native): $M_1 = W$
  - Measurement 2 (enhanced): $M_2 = W + 0.5\,X$
  - Estimated iodine: $2\,(M_2 - M_1)$ Variance = 4 (Var M_2 + Var M_1) = 8 N^2
  - Estimated soft tissue: M_1 Variance = Var M_1 = N^2

VNC and iodine noise (standard deviation) in DECT are about twice as high as in subtraction imaging.

This toy example assumes iodine to contribute half as much to the gray value for the high kV scan as for the low kV scan.
Dose is assumed to be the same in both scenarios.

Materials

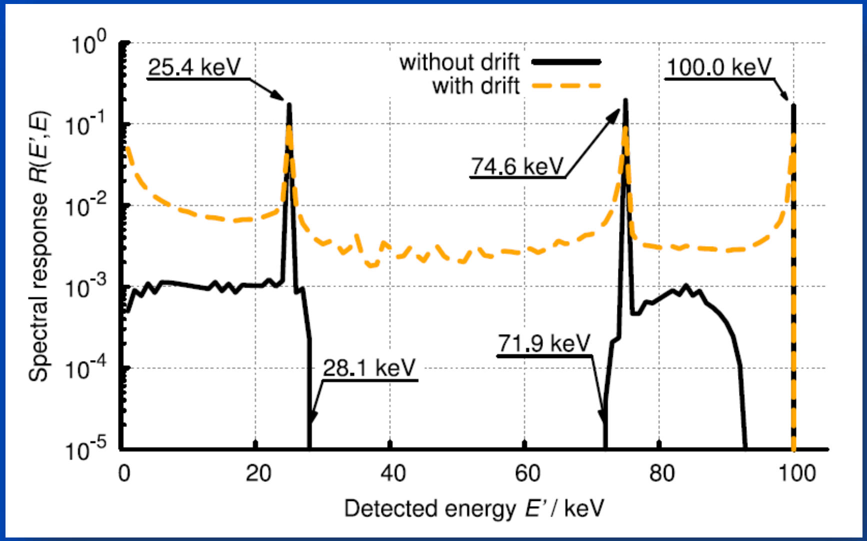

- Simulations only
- Emitted spectra
  - Tube current *I*, no TCM
  - Tube voltage *U*, from 70 kV to 150 kV
  - 0, 1, 2 or 3 mm Cu patient-specific prefilter (PSP)[1]
  - Tucker spectrum filtered by 1 mm Al + 0.9 mm Ti
- Three phantom sizes

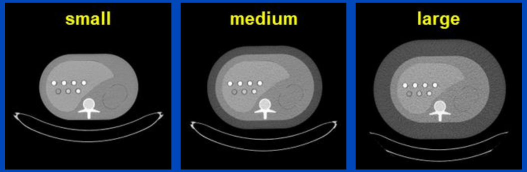

- Detected spectra
  - Photon-counting detector, 1.6 mm CdTe
  - Realistic spectral response[2]
  - Up to $B = 4$ energy bins
  - Threshold positions $T_b \in \{20, 33, 50, 61, 65, 70, 81, 91, 100, 120\}$ keV

I Gd Yb Hf W Au Bi

6472^S parameter combinations for S scans.

(here S = 2 or 3)

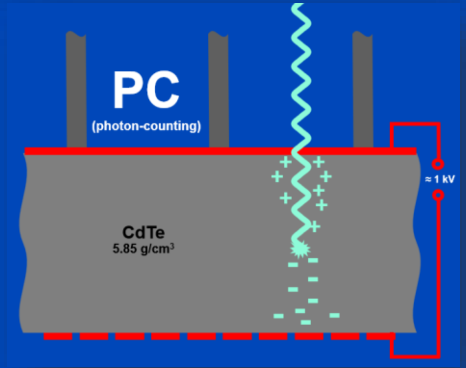

- Dose = $\text{CTDI}_{32\text{ cm}} = \kappa(U)\cdot I$
- Optimized image domain material decomposition[3]
  - H_2O, I, Gd, Yb, Hf, W, Au, Bi

$$g(\boldsymbol{r}) = \boldsymbol{w}^{\mathrm{T}} \cdot \begin{pmatrix} f_1(\boldsymbol{r}) \\ \vdots \\ f_B(\boldsymbol{r}) \end{pmatrix}$$

[1]Using a 2 mm Cu prefilter approximately corresponds to 0.6 mm Sn or to 0.5 mm Ag.
[2]S. Faby, M. Kachelrieß et al. Med. Phys. 43(7):3945-3960, July 2016.
[3]S. Faby, M. Kachelrieß et al. Med. Phys. 42(7):4349-4366, July 2015.

W+WX vs. WX+WX with B = 1 for X = Iodine

Two separate scans necessary → W+WX

Preferrably to be realized with DSCT. → WX+WX
Can also be done with other DECT implementations, but then won't have PSP.

200 mm, real X=Iodine	Scenario 1 80/140 kV, no PSP	Scenario 2 70/150 kV, PSP	Scenario 3 opt., PSP
W+WX	311 HU, 0 HU 27.8, 6.07, 6.51	366 HU, 0 HU 25.9, 6.58, 7.05	370 HU, 0 HU 33.8, 8.43, 9.04
WX+WX	311 HU, 203 HU 8.11, 2.11, 2.26	366 HU, 88 HU 19.1, 5.00, 5.34	370 HU, 89 HU 21.1, 5.72, 6.09
Penalty	11.7, 8.25, 8.31	1.84, 1.73, 1.74	2.56, 2.17, 2.20

400 mm, real X=Iodine	Scenario 1 80/140 kV, no PSP	Scenario 2 70/150 kV, PSP	Scenario 3 opt., PSP
W+WX	269 HU, 0 HU 3.73, 0.67, 0.72	323 HU, 0 HU 3.93, 0.77, 0.82	328 HU, 0 HU 4.27, 0.89, 0.96
WX+WX	269 HU, 161 HU 1.26, 0.27, 0.29	323 HU, 79 HU 2.82, 0.58, 0.62	328 HU, 79 HU 3.19, 0.67, 0.72

All images reconstructed at same spatial resolution. X = Iodine. Triples are SNRDs of W, X, and $SNRD_{tot}$. PSP = patient-specific prefilter.

Conclusions on W+WX vs. WX+WX with $B = 1$ for X = Iodine

- If no PSPs are available there is an enormous dose penalty of doing WX+WX:
  - **roughly 8× dose penalty** if only 80 kV to 140 kV but no PSPs are available.
  - **roughly 2× dose penalty** if 70 kV, 150 kV and PSPs are available.
- The findings are valid across all patient sizes.

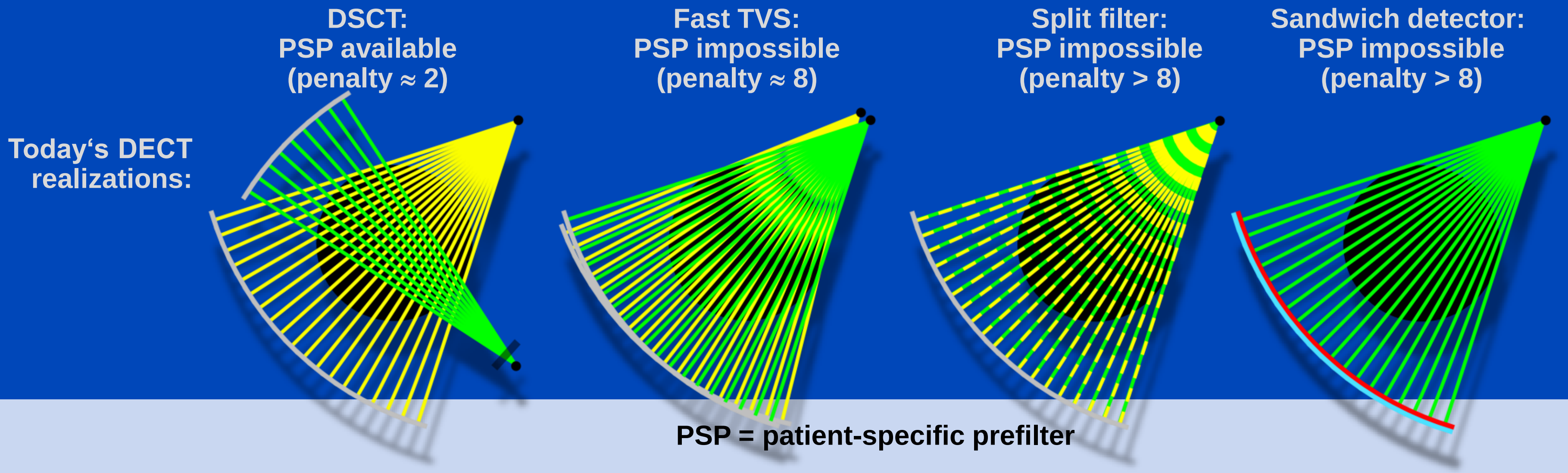

PSP = patient-specific prefilter

X=Iodine plus Another Contrast Agent Y

400 mm, real	Y=Gadolinium	Y=Hafnium	Y=Bismuth	
WXY	0.74, 0.25, 0.17, 0.20	1.40, 0.38, 0.27, 0.33	0.89, 0.25, 0.24, 0.26	3
W+WXY	2.02, 0.41, 0.33, 0.38	2.67, 0.48, 0.43, 0.48	2.37, 0.34, 0.39, 0.38	2
WXY+WXY	1.69, 0.42, 0.29, 0.36	1.54, 0.51, 0.31, 0.39	1.58, 0.43, 0.31, 0.37	3
WX+WXY	1.75, 0.49, 0.48, 0.51	1.90, 0.33, 0.80, 0.48	2.13, 0.38, 0.62, 0.48	1
WY+WXY	1.80, 0.52, 0.43, 0.49	1.57, 0.73, 0.29, 0.43	1.39, 0.74, 0.26, 0.41	1
WX+WY	2.09, 0.35, 0.44, 0.41	2.11, 0.35, 0.45, 0.41	2.13, 0.36, 0.36, 0.38	2
W+WX+WY	4.46, 0.73, 0.72, 0.78	4.28, 0.73, 0.73, 0.79	4.40, 0.66, 0.63, 0.69	2
W+WX+WXY	3.14, 0.72, 0.72, 0.77	3.59, 0.77, 0.76, 0.82	3.85, 0.69, 0.67, 0.73	1
W+WY+WXY	3.79, 0.74, 0.74, 0.79	3.98, 0.77, 0.76, 0.82	4.29, 0.64, 0.63, 0.68	1
W+WXY+WXY	2.26, 0.42, 0.34, 0.39	3.12, 0.61, 0.57, 0.63	3.48, 0.48, 0.45, 0.49	2
WX+WXY+WY	3.06, 0.75, 0.75, 0.80	3.52, 0.72, 0.71, 0.77	3.61, 0.73, 0.71, 0.77	0
WX+WX+WXY	2.72, 0.61, 0.65, 0.67	2.80, 0.61, 0.73, 0.69	2.79, 0.58, 0.58, 0.62	1
WY+WY+WXY	2.67, 0.64, 0.54, 0.61	1.73, 0.74, 0.37, 0.50	1.57, 0.62, 0.31, 0.41	1
WXY penalty	$(0.80/0.20)^2 = 15.5$	$(0.82/0.33)^2 = 6.28$	$(0.77/0.26)^2 = 8.91$	
WXY+WXY penalty	$(0.80/0.36)^2 = 5.05$	$(0.82/0.39)^2 = 4.52$	$(0.77/0.37)^2 = 4.37$	

Highlighted (white) are those scan strategies that come with an $SNRD_{tot}$ dose penalty of at most 20%. Quadruples are SNRDs of W, X, Y, and $SNRD_{tot}$.

dkfz.

Conclusions

- **Investing into <u>motion correction</u> and <u>multi-scan strategies</u> would be highly beneficial:**
  - **Reduces patient dose by at least 50% for the one-agent task.**
  - **Reduces patient dose by more than 90% for the two-agent task.**
- **Limitation:**
  - **Simulation study only**

Thank You!

- This study was supported in part by the Helmholtz International Graduate School for Cancer Research, Heidelberg, Germany.

- This presentation will soon be available at www.dkfz.de/ct.
- Job opportunities through DKFZ's international PhD or Postdoctoral Fellowship programs (marc.kachelriess@dkfz.de).

- Parts of the projection simulation software and of the image reconstruction software were provided by RayConStruct® GmbH, Nürnberg, Germany.